



# A Simple Approach for the Synthesis of Cellulose Nanofiber Reinforced Chitosan/PVP Bio Nanocomposite Film for Packaging

Ritesh Kumar<sup>1</sup> · Bhuvneshwar Rai<sup>2</sup> · Gulshan Kumar<sup>1</sup>

Published online: 16 October 2019  
© Springer Science+Business Media, LLC, part of Springer Nature 2019

## Abstract

The development of chitosan-based food packaging film has been increasing due to its wider availability, biodegradability, low-cost, and renewability. The purpose of this study was to develop cellulose nanofibers (CNFs) reinforced Chitosan/PVP(CHP) green bio nanocomposite film by solvent casting method with enhanced barrier and mechanical property. CNFs of dimension 9–11 nm and 100–200 nm were extracted from jute fibers by directly treating it with HNO<sub>3</sub>–NaNO<sub>2</sub> mixture. Bio nanocomposite films were synthesized with various concentrations of CNFs and evaluated using SEM, TGA/DTG and XRD to analyze the morphology, thermal behavior and crystallinity of bio nanocomposite films. SEM analysis revealed the uniform dispersion of CNFs in CHP matrix. Thermal stability of prepared bio nanocomposite films was improved with the loading of 5 wt% of cellulose nanofibers. ATR(FT-IR) spectra shows physical interaction between all the components of bio nanocomposite film. The bio nanocomposite films were also characterized for physical property like thickness, mechanical testing and barrier properties. The addition of CNFs significantly enhanced the mechanical property of bio nanocomposite films. Furthermore, water and oxygen transmission rate of bio nanocomposite film decreased with the increase in CNFs concentration. Overall the performed studies confirmed, the use of CNFs in polymer matrix makes it possible to produce a flexible, transparent, thermally stable bio nanocomposite film with enhanced mechanical and barrier properties for food packaging applications.

**Keywords** Jute fiber · Cellulose nanofibers · Bio nanocomposite film · Food packaging

## Introduction

Petroleum derived plastic materials exhibited tremendous benefits to the society in terms of diversified applications in textiles, healthcare products, packaging and toys. Packaging industry is a bigger consumer of plastic material for food packaging application, but the excessive use of plastic material has resulted in the production of harmful chemicals and in addition contribute to uncontrolled growing landfills [1]. Thus, biodegradability and renewability have become an essential requirement for plastic material to be used for any applications. Recently many academic and

industrial groups are interested to develop green biodegradable plastic material derived from renewable resources to replace petroleum-based polymer i.e., oil based counterpart [2–6]. In this context natural biopolymer such as cellulose [2], starch [7], chitosan [8], collagen [9], alginate [10] have been used instead of petroleum-based polymer because of their abundant, renewable, eco-friendly and specific properties [11]. Chitosan is an amino polysaccharide derived from deacetylation of chitin, which is the second most abundant polymer after cellulose. Owing to its biocompatibility, antimicrobial, biodegradability, and excellent film-forming capability, [12–14] chitosan based material play an active role in biodegradable plastic for making packaging material to protect the food from microbial attack and contamination and also increase the shelf life of food [15]. Apart from this it has been also used in various application such as tissue engineering, wound healing, drug delivery, waste water treatment, cosmetics, food science and others [16]. Despite of above-mentioned advantages with chitosan, it possesses some limitations like poor mechanical, thermal,

✉ Gulshan Kumar  
gulshandhamija@ipu.ac.in

<sup>1</sup> University School of Basic and Applied Sciences, Guru Gobind Singh Indraprastha University, New Delhi 110078, India

<sup>2</sup> Material Science Division, Shriram Institute for Industrial Research, 19 University Road, New Delhi 110007, India

and barrier property which limit its use in many practical applications [17]. Several approaches have been reported by different researchers to enhance the properties of chitosan, most appropriate of them are cross-linking method or blending with another polymer(s) [18]. As chitosan contains large number of OH and  $\text{NH}_2$  group in its chain which acts as reactive sites to bind with other biopolymers leading to enhancement in its properties [19]. Polyvinylpyrrolidone (PVP), a water-soluble, non-toxic, biocompatible synthetic polymer is utilized in medical, health-related domains, cosmetic, drug delivery, tissue engineering and wound dressing. It is reported that PVP act as crosslinker and forms hydrogen bond with chitosan and consequently increases its thermal and mechanical property [20]. Yeh et al. reported the blend of chitosan and PVP, at a different ratio to prepare a new material which has enhanced property rather than pristine chitosan and PVP alone [21]. The blend of chitosan and PVP polymer has been widely used in biotechnology and chemical technology [20, 22]. However, Li et al. reported that the blending of PVP with chitosan at high concentration does not significantly affect the chemical and physical properties of chitosan. Moreover, PVP is a low-cost synthetic polymer as compared to chitosan biopolymer so the blending of PVP with chitosan reduces the cost of a chitosan-based film [23]. Further, different group of researchers are working on the improvement of properties of chitosan by blending it with natural inorganic fillers such as nano-clay [24], titanium dioxide [25], silver nanoparticles [16], etc. But blending of chitosan with natural inorganic fillers is very difficult task due to the difference in their structure, chemical nature as well as density.

In recent years nanocellulose obtained from natural fiber is finding application as reinforcing agent in polymer matrix for use in various applications such as drug delivery, wound dressing, Packaging, etc.[26, 27]. These unique properties such as high elasticity, biodegradability, low-cost, water holding capacity, mechanical strength and thermal stability [28–30] of the nanocellulose are responsible for their diversified applications [31]. Dehnad et al. prepared chitosan-nanocellulose biocomposites for extending shelf life of ground meat [32]. Cellulose nanofibers and chitosan biopolymer show good compatibility with each other because of the structural similarity, which results in an improvement in thermal, mechanical, and barrier property of polymer [33].

Recently cellulose nanofibers have been isolated from jute fiber by treating it with  $\text{HNO}_3$ – $\text{NaNO}_2$  mixture. This oxidation process converts primary alcohol into aldehyde or carboxylate groups. The prepared cellulose nanofibers had width and length in the range of 9–11 nm and 100–200 nm. The negatively charged carboxylate group of cellulose nanofibers and positively charged ammonia groups ( $\text{NH}_3^+$ ) of chitosan are responsible for the strong interaction between reinforcement and polymer matrix [34].

However, to the best of knowledge, there is no literature about the blending of  $\text{HNO}_3$ – $\text{NaNO}_2$  oxidized CNFs, chitosan and PVP for producing bio nanocomposite film with enhanced properties for packaging application.

The research work aims to develop high performance bio nanocomposite film based on CHP matrix reinforced with cellulose nanofibers through solvent casting method with improved properties for packaging. The developed bio nanocomposite films were evaluated for thermal stability, crystalline nature, mechanical property, optical and barrier properties.

## Experimental Details

### Materials

Chitosan (low molecular weight, off white to yellow-beige powder/chips), Polyvinylpyrrolidone K-30(PVP). Jute fibers procured from the Surya Prakash & company Jaipur (India) were used in the study. Nitric acid (67%), sodium nitrite (97%), ethanol, acetone, acetic acid of analytical grade was procured from fisher scientific and were used without further purification. Double distilled water was used throughout the experiment.

### Preparation of Cellulose Nanofibers

The CNFs were isolated from jute fiber by following modified procedure [35, 36]. Chopping of jute fibers was carried-out using kitchen grinder for 30 min to reduce length of the fibers approx. 1 mm. 1 gm of chopped jute fibers were taken in 250 ml three neck round bottom flask containing 14 ml (0.2 mol) nitric acid. The fibers were completely soaked in the nitric acid and then 1.96 gm (0.02 mol) sodium nitrite was added into it. The mouth of the flask was sealed with a stopper to prevent the red fumes formed inside the flask. The flask was kept at 60 °C for 10 h to complete the reaction. After completion of the reaction, 100 ml distilled water was added into it to quench the reaction. The solution was kept for 1 h at room temperature for equilibration. Then the solution was centrifuged at 3000 rpm for 15 min to separate the excess acid from it. The washing was carried out by centrifuging with 2:1 ethanol/water mixture at 3000 rpm and the process was repeated till pH becomes neutral. CNFs were separated from ethanol–water mixture, then 50 ml distilled water was added into it and stored in centrifuge tube at 4 °C till used. Under this reaction condition the yield of CNFs was ~22–23 wt% (based on original weight of raw fiber).

## CHP/CNFs Nanocomposite Film Preparation

Solvent casting method was used to prepare nanocomposite film. Figure 1 shows the schematic for the preparation of CHP/CNFs nanocomposite film. Briefly, 1.0 gm (1%w/v) of chitosan was dissolved in 1N acetic acid solution (100 ml) by continuous stirring for 5 h. PVP (0.250 gm) powder was subsequently added to chitosan solution (in respect to the dry weight of chitosan). The solution was centrifuged for 10 min at 3000 rpm to remove the insoluble polymeric particles and to burst small air bubbles formed during stirring.

1, 3 and 5 wt% of CNFs (with respect to the weight of chitosan) was dispersed in 10 ml distilled water and sonicate it for 30 min. Dispersed CNFs were added to polymeric solution with continuous stirring for 16 h followed by sonicating the solution for half an hour. The resulting solution was poured into the petri dish and dried in hot air oven at 60 °C for 12 h.

Dried composites were peeled off from the petri dish and stored in desiccator at room temperature for further use. The nanocomposite films were coded as CHP/CNFs 0%, CHP/CNFs 1%, CHP/CNFs 3%, CHP/CNFs 5%.

## Transmission Electron Microscopy (TEM)

Synthesized CNFs were analyzed using TEM (Model: TECNAI 200 kV TEM, make: Fei, Electron Optics) at an accelerating voltage of 80 kV, to determine the morphology and size. To record the TEM of the CNFs sample, a drop of 0.1 wt% dilute suspension was deposited on the surface of a clean carbon coated Cu grid and negative staining with 2 wt% aqueous uranyl acetate solution to

get better contrast image of the sample and dried at room temperature before recording TEM image.

## Thickness of Nanocomposite

Thickness of prepared bio nanocomposite films were determined using hand-held digital micrometer. For each specimen 10 random positions were measured and the average value was taken as the thickness of polymer nanocomposite.

## Scanning Electron Microscopy (SEM)

Surface topology of prepared bio nanocomposite films were determined using SEM (Model: EVO 18, Make: ZEISS Research Microscopy Solutions) at accelerating voltage of 20 kV. To record the SEM, samples were coated with a layer of gold.

## X-Ray Diffraction (XRD)

X-ray diffraction pattern of prepared bio nanocomposite films were analyzed using X-ray diffraction instrument (Model: Miniflex PDXL, Make: Rigaku). To measure the XRD pattern, CuK $\alpha$  radiation of wavelength,  $\lambda$  0.15406 nm generated at 40 kV and 30 mA. Data collection was carried out in the range of  $2\theta$  varying from 0° to 50° with a scanning speed of 6°/min.

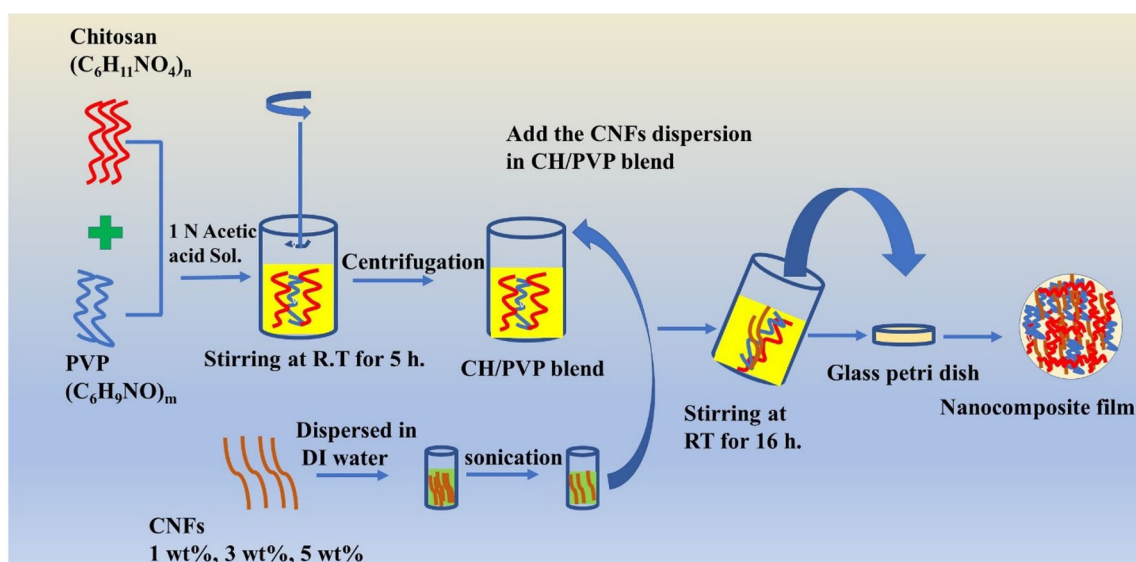


Fig. 1 Schematic for the preparation of CNFs loaded bio nanocomposite film

## Attenuated Total Reflectance-Fourier Transform Infrared Spectroscopy (ATR-FTIR)

Chemical structure of developed bio nanocomposite films was determined using (ATR-FTIR) spectrophotometer (Model: Nicolet iS5N Make: Thermo Fisher Scientific) in transmission mode between 400 and 4000  $\text{cm}^{-1}$  at scanning speed 32 scans/s with a resolution of 4  $\text{cm}^{-1}$ .

## Optical Transmittance

Transmittance spectra of bio nanocomposite films were recorded in the range of 200–800 nm wavelength using UV-Vis spectrophotometer (Model: double beam spectrophotometer U-2900/2910 Make: HITACHI). The air was used as the reference during measurement.

## Gel Swelling Study

The nanocomposite films were previously dried and then immersed in distilled water at 25 °C until equilibrium was not reached. The sample were weighed at regular interval of time until the equilibrium state was not reached. The swelling behavior of nanocomposite films were calculated according to the equation:

$$\text{Swelling (\%)} = (W_s - W_d) / W_d \times 100$$

$W_s$  is the weight of wet sample and  $W_d$  is the weight of dry sample.

## Contact Angle Analysis

Hydrophilicity of prepared nanocomposite films were analyzed using Drop Shape Analyzer (Model: DSA25 Make: Kruss). Briefly, 3  $\mu\text{l}$  droplet of di-iodomethane was dropped on (2 × 2 cm) composite sample using automated micro syringe system. Measurement was performed at room temperature by taking average and standard deviation of three different locations of sample.

## Water Vapor Transmission Rate (WVTR)

Water vapor transmission rate of developed nanocomposite films were measured by gravimetric technique according to the ASTM E 96/E 96M-05 (Water method). To measure WVTR, bio nanocomposite films were sealed over the mouth of test cup (diameter 76 mm) containing 25 ml of water. Then the test cup was placed in controlled temperature and relative humidity (RH) chamber at the temperature of (32 ± 2) °C and relative humidity of (50 ± 2) % and 0.02–0.3 m/s of air. Three replicas of each specimen were

measured and weighed at regular interval of time. Weight loss vs time plot was constructed and from slope of the plot, WVTR was calculated as follow

$$\text{WVTR} = \text{Slope} \times 24 / A [\text{g}/\text{m}^2/\text{day}]$$

where A represent permeation area of sample.

## Oxygen Permeability

Oxygen transmission rate of nanocomposite films were analyzed by Gas permeability tester (Model: VAC-VBS, make: Labthink) using ASTM D1434 standard at 29 °C in relative humidity of 41.7%. Total of four specimens were prepared for each sample to measure oxygen transmission rate. Oxygen permeability (OP) of nanocomposite was determined by multiplying oxygen transmission rate by the film thickness and divided it by  $\Delta P$  (partial pressure across the composite).

$$\text{OP} = (\text{OTR} \times l) / \Delta P$$

where  $l$  is the thickness of nanocomposite and  $\Delta P$  is the partial pressure across the composite.

## Thermal Gravimetric Analysis (TGA/DTG)

Thermal behavior of nanocomposite films was studied by using TGA instrument (Model: STA 449F3, Make: NETZSCH) at heating rate of 10 °C/min under constant nitrogen flow. To understand the behavior of material under temperature both the TGA and DTG curve were recorded.

## Mechanical Properties

Tensile testing of nanocomposite films was carried out by Universal testing machine (Model: 1121, Make: INSTRON) with a load cell of 30 kN according to ASTM D-638-2010 standard with a cross head speed of 1mm/s at room temperature. The dimensions of sample were 1 cm × 8 cm in rectangular shape with the gauge length of 5 cm. The testing was performed at room temperature.

## Biodegradability Study

Biodegradability study of nanocomposite films were performed by exposing the samples to compost. 2 × 2 cm piece of nanocomposite was put in compost at 4–6 cm depth at room temperature. At selected time interval samples were taken out from the compost, washed with distilled water, dried it at room temperature and stored in desiccator till weight becomes constant. Based on the initial and final weight before and after degradation the average weight loss percentage for each sample was calculated.

## Results and Discussion

### Characterization of Cellulose Nanofibers

#### Morphological Study of CNFs

The size and morphology of CNFs obtained from jute fiber was examined using TEM and SEM at the nanoscale and shown in Fig. 2 at different magnification. TEM photographs (Fig. 2a, b) shows the needle like shape of CNFs. The width and length of CNFs were measured using Image J software, which shows the diameter of CNFs in the range of 9–11 nm and length in the range of 100–200 nm. SEM was also used to examine the size and morphology of CNFs, it shows the network structure of entangled fibrils and diameter in the nano range (Fig. 2c). Figure 2d shows the size distribution histogram obtained through the particle size analysis test for CNFs. Narrow size distribution of cellulose nanofibers is a very important aspect of nanomaterial to enhance the properties of polymer matrix. The strong interaction between CNFs, PVP and chitosan be likely due to the presence of oxygen and nitrogen groups of PVP and chitosan. These groups also involve in stabilizing CNFs and prevent the agglomeration of CNFs in CHP matrix [37, 38].

### Characterization of Film

In order to enhance the property of CHP composite some additives or fillers are necessary to introduce into it. The incorporation of cellulose nanofibers in CHP matrix produced the transparent and flexible nanocomposite film and also neglect the chance of contraction after drying.

#### Film Thickness

CNFs loaded nanocomposite films were slightly thicker compared to pristine CHP film. Thickness of pristine CHP film was 146  $\mu\text{m}$  while CHP/CNF 1%, CHP/CNF 3% and CHP/CNF 5% were 148, 150 and 157  $\mu\text{m}$ .

#### Scanning Electron Microscopy

Scanning electron microscopy was used to analyze the surface morphology of bio nanocomposite film with and without loading of CNFs at different magnification. In this study we used PVP as the crosslinker because it shows good compatibility with chitosan biopolymer, safer to be used in cosmetic, biomedical and food products etc. Crosslinking of PVP and chitosan enhance the thermal, chemical and mechanical properties of prepared composite film, it also increases flexibility of the film. Secondly, PVP is a low-cost synthetic polymer which reduce the cost of preparation of

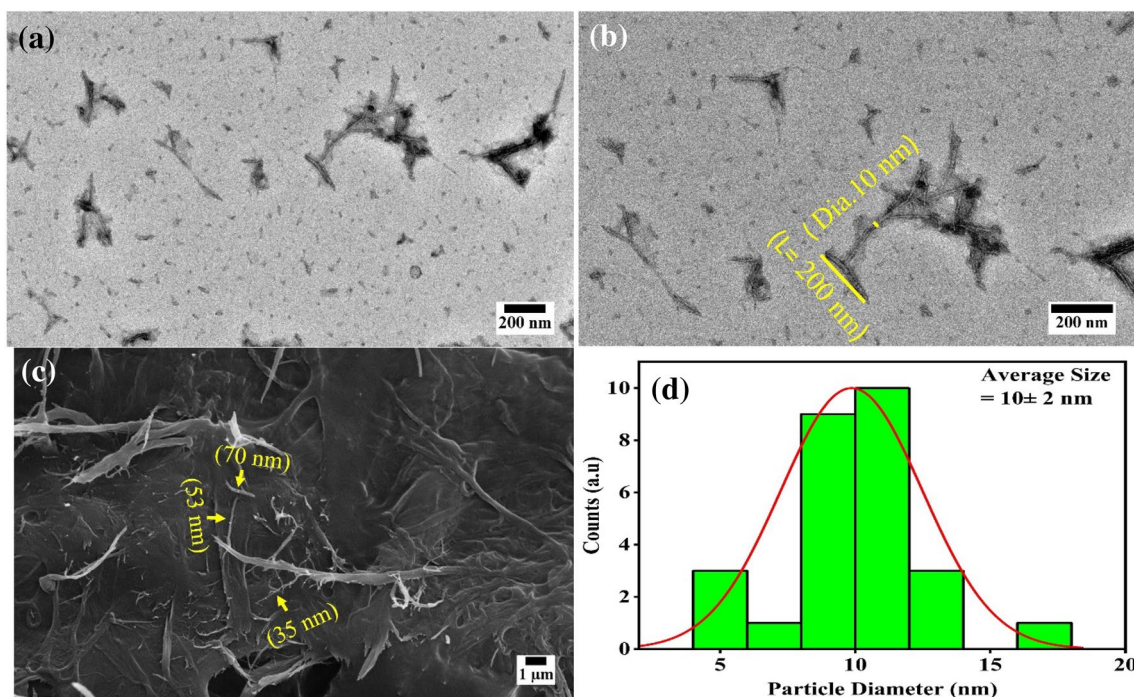


**Fig. 2** a, b TEM image of CNFs at different magnification c SEM image of CNFs d Histogram of CNFs (Particle size was calculated by image J software from the TEM image)

composite film [34]. Figure 3a shows the SEM image of CH/PVP(CHP) composite and its smooth or even surface confirms the homogeneous mixing of chitosan and PVP. However, with the addition of 1%, 3%, 5% CNFs into CHP matrix, increased the roughness of developed nanocomposite film. Thus, it confirmed the uniform distribution of CNFs in matrix and shows the excellent compatibility between CNFs and CHP matrix. The CHP matrix and CNFs shows good compatibility with each other due to the formation of strong hydrogen bonding between C=O, NH<sub>2</sub> and C=O group of PVP, chitosan and CNFs [37, 38].

### X-Ray Diffraction

The XRD was performed to determine the crystallinity of prepared bio nanocomposite films. Figure 4 shows the XRD pattern of CHP/CNFs 0%, CHP/CNFs 1%, CHP/CNFs 3% and CHP/CNFs 5% nanocomposite film. X-ray diffraction of CHP shows diffraction peaks at 9.22° and 20.15°. CNFs loaded nanocomposite with different concentrations shows almost the same diffraction pattern such as  $2\theta = 9.22^\circ$ , 11.22°, 18.15°, 22.82° respectively and results are depicted in Fig. 4. Diffraction pattern of CNFs loaded nanocomposite film shows superimposed peaks of chitosan and CNFs in the range of 20–25° and cannot be distinguished separately. The broad diffraction peaks attribute to the amorphous nature of CHP/CNFs nanocomposite film [22, 38, 39].

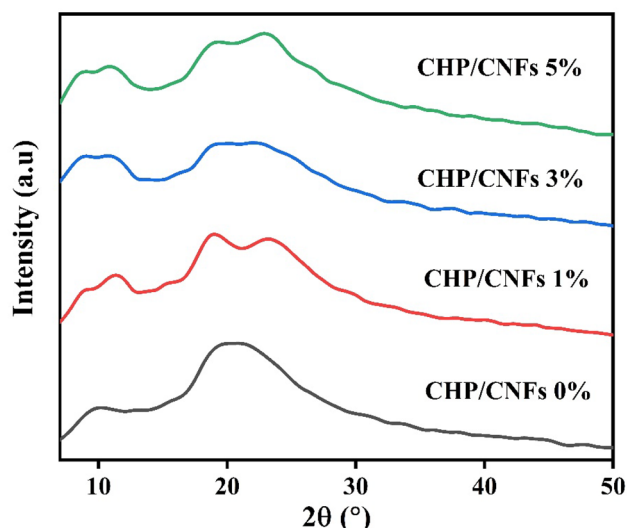


**Fig. 4** XRD pattern of CHP/CNFs 0%, CHP/CNFs 1%, CHP/CNFs 3%, and CHP/CNFs 5% bio nanocomposite film

### FT-IR Spectroscopy

Attenuated total Reflectance-Fourier transform infrared spectroscopy recorded to analyze the molecular group involved in uniform distribution of CNFs in CHP polymeric matrix. Figure 5 shows the ATR-FTIR spectra of pristine CHP film and CHP/CNFs nanocomposite with various

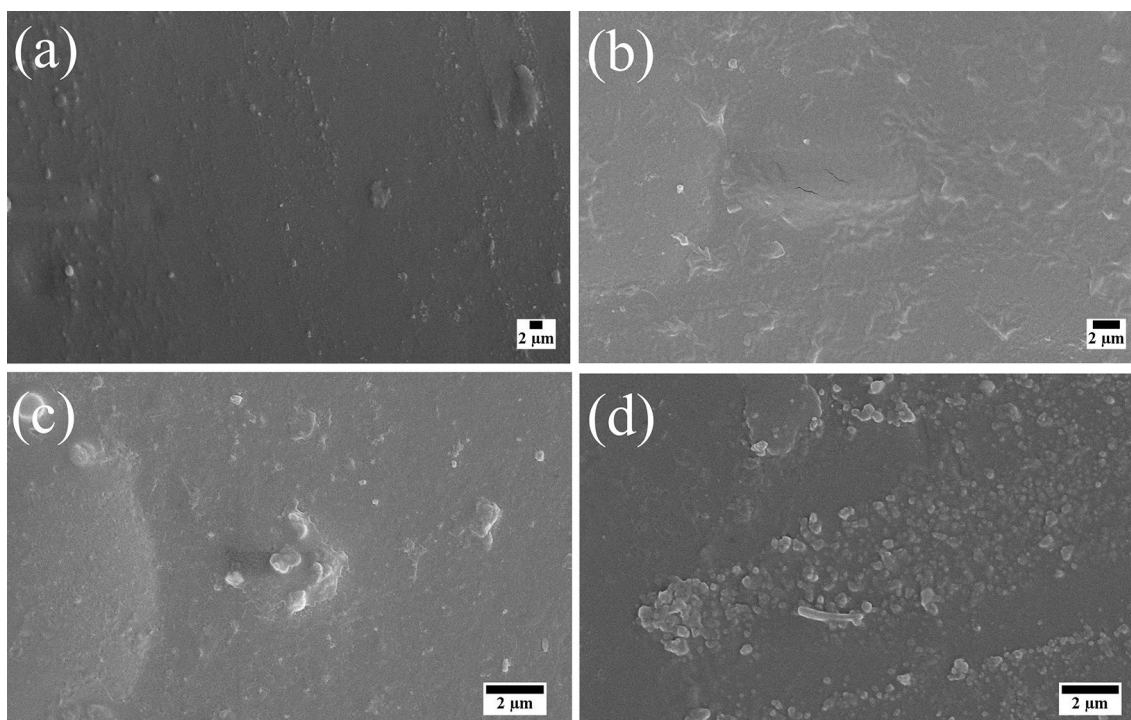


**Fig. 3** SEM image of **a** CHP/CNFs 0% **b** CHP/CNFs 1% **c** CHP/CNFs 3% **d** CHP/CNFs 5%

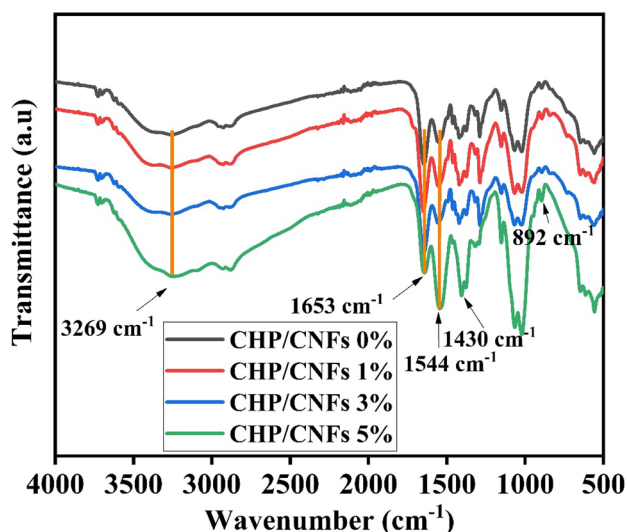


**Fig. 5** ATR (FT-IR) Spectra of CHP/CNFs 0%, CHP/CNFs 1%, CHP/CNFs 3%, and CHP/CNFs 5% bio nanocomposite film

concentration of CNFs. As shown in Fig. 5 peak position at  $1653\text{ cm}^{-1}$  and  $3269\text{ cm}^{-1}$  related to the C=O and OH group of chitosan and peak position at  $1014\text{ cm}^{-1}$  related to C–N stretch and  $1415\text{ cm}^{-1}$ ,  $1544\text{ cm}^{-1}$  assigned to the vibration of pyrrolidone ring of PVP. CHP/CNFs nanocomposite shows some additional peak of CNFs at  $1430\text{ cm}^{-1}$  related to the  $\text{CH}_2$  bending vibration (Crystalline peak of cellulose) and  $892\text{ cm}^{-1}$  corresponds to the C–O–C pyranose ring of cellulose (amorphous band of cellulose). From the observations, it concluded that FT-IR spectra of all the prepared nanocomposite films are almost same. This may be due to the addition of very small fraction of CNFs into CHP matrix [19, 37, 38, 40, 41].

### UV–Vis Spectroscopy

UV–Visible spectroscopy used to analyze the optical transparency of pristine CHP film and CHP/CNFs bio nanocomposite films by recording the transmittance spectra in UV–Vis region (200–800 nm). The transmittance spectra of pristine CHP film and CHP/CNFs nanocomposite films with various concentrations of CNFs are shown in Fig. 6. The transmittance of Pristine CHP film and CNFs loaded nanocomposite films shows a transmittance of approx. 90%. Thus, it indicated that the loading of CNFs into CHP matrix does not affect the transmittance property of developed bio nanocomposite films and it confirmed the uniform dispersion of CNFs. It also confirmed that all the components of nanocomposite have excellent compatibility so, visible light can be easily transmitted through bio nanocomposite films. Indeed, highly transparent bio nanocomposite film can be

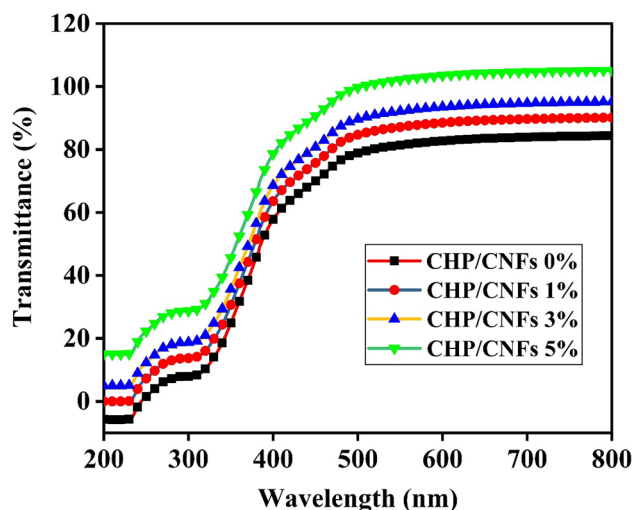


**Fig. 6** UV–Vis Spectra of CHP/CNFs 0%, CHP/CNFs 1%, CHP/CNFs 3%, and CHP/CNFs 5% bio nanocomposite film

used as a transparent film for food packaging applications [31].

### Gel Swelling Study

Figure 7 illustrates the swelling percentage and water uptake of pristine CHP film and CHP/CNFs nanocomposite film in distilled water at room temperature for different time period. The effect of different concentration of CNFs loading on water uptake and swelling percentage with respect to time was analyzed and shown in Fig. 7. There are many factors responsible for the water uptake and swelling percentage such as stiffness, hydrophilicity

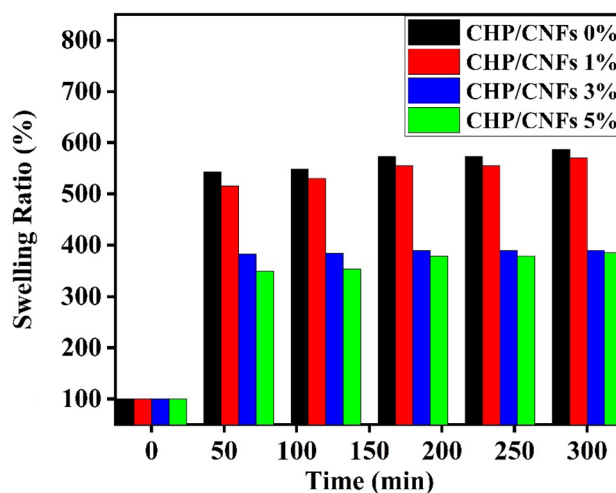


**Fig. 7** Swelling percentage of CHP/CNFs 0%, CHP/CNFs 1%, CHP/CNFs 3%, and CHP/CNFs 5% bio nanocomposite film

and pore size of nanocomposite. Increase in swelling of composite with time shows the swelling of polymer matrix due to water uptake which is responsible for the weakening of hydrogen bond between CH-PVP-CNFs. Chitosan bio polymer shows swelling due to the ionization and protonation of carboxyl and amino groups, respectively. PVP is also responsible to increase the swelling of composite. Swelling behavior of nanocomposite film depends on the interaction of fillers and matrix. Swelling behavior of bio nanocomposite film decreased with the incorporation of CNFs. 3% and 5% CNFs loaded nanocomposite film shows decrease in water uptake than pristine CHP composite. This is due to high crystallinity of CNFs which is less hydrophilic compared to CHP matrix and also due to an increase in the hindrance of crystal at higher loading [22, 42].

### Contact Angle Measurement

Contact angle measurement used to analyze the hydrophilicity or hydrophobicity of polymeric film. Figure 8 shows the contact angles of pristine CHP film and CHP/CNFs nanocomposite film loaded with various concentrations of CNFs. PVP polymer is hydrophilic in nature and the presence of this polymer in matrix increase the hydrophilicity of matrix and hence decreases the contact angle of the film. Moreover, loading of CNFs in CHP matrix is also responsible for the decrease in contact angle of nanocomposite films. This is probably due to the presence of polar group OH on the surface of CNFs which may increase the distance between carbon chain in chitosan results in decrease in contact angle [41].

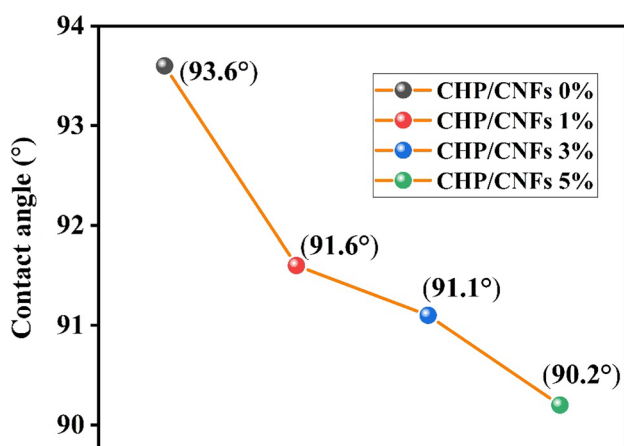


**Fig. 8** Average contact angle value of CHP/CNFs 0%, CHP/CNFs 1%, CHP/CNFs 3%, and CHP/CNFs 5% bio nanocomposite film

### Water Vapor Transmission Rate

The knowledge of water vapor transmission rate is a necessary feature in packaging applications. Figure 9 shows the water vapor transmission rate of pristine CHP film and CNFs reinforced bio nanocomposite films. With the addition of CNFs of various concentration in CHP matrix, resulted bio nanocomposite films shows decrease in water vapor transmission rate as compared to pristine CHP film. The WVTR of CHP/CNFs 0% composite was 1086.04 gm/m<sup>2</sup>/day which decreased significantly after incorporation of CNFs. The WVTR of CHP/CNFs 1%, CHP/CNFs 3%, CHP/CNFs 5% was 992.08, 990.69 and 975.45 gm/m<sup>2</sup>/day. The decrease in WVTR values was probably due to the closure of surface pores and surface densification of CHP matrix with the addition of cellulose nanofibers. CNFs act as an impermeable barrier, which increases the path length of gas diffusion and also resulted in decrease in water vapor transmission rate of bio nanocomposite. This result also shows the uniform dispersion of CNFs in CHP matrix [22, 34].

### Oxygen Permeability Study

Oxygen permeability of pristine CHP film and with various concentration of CNFs reinforced bio nanocomposite films are shown in Fig. 10. Oxygen permeability is the volume of oxygen passing through polymer nanocomposite per unit area in unit time under predefined temperature, relative humidity and oxygen partial pressure. Transmission of oxygen from environment to CHP/CNFs bio nanocomposite may affect the shelf life of it. CNFs loaded bio nanocomposite film shows improved barrier to oxygen compared to pristine CHP film. Bio nanocomposite films with 5% loading of CNFs shows excellent barrier properties. SEM results shows the uniform distribution of cellulose nanofibers in polymer

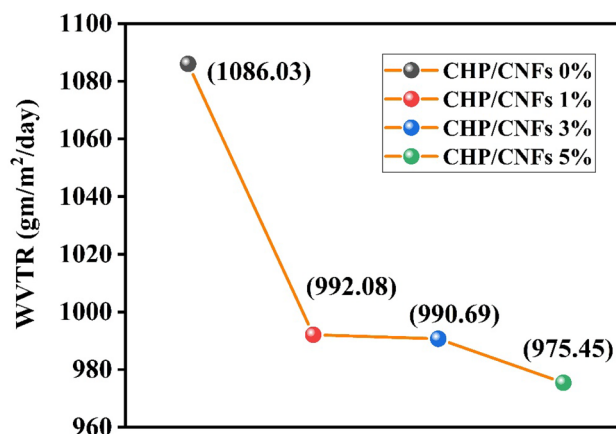


**Fig. 9** Water vapor transmission rate of CHP/CNFs 0%, CHP/CNFs 1%, CHP/CNFs 3%, CHP/CNFs 5% bio nanocomposite film



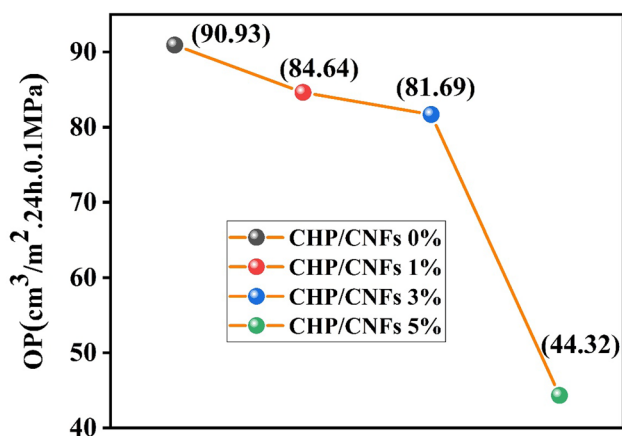


Fig. 10 Oxygen permeability of CHP/CNFs 0%, CHP/CNFs 1%, CHP/CNFs 3%, CHP/CNFs 5% bio nanocomposite film

matrix therefore strong interaction will take place between CHP and CNFs resulting in a compact structure which prevents the permeation of oxygen through the film [22, 34].

### Thermogravimetric Analysis (TGA/DTG)

Mean integral (TGA) and derivative (DTG) thermogravimetric analysis used to analyze the thermal stability of CHP and cellulose nanofibers loaded CHP/CNFs nanocomposite with the increase in temperature under continuous nitrogen flow. The weight loss versus change in temperature of pristine CHP film and CNFs reinforced nanocomposite films are shown in Fig. 11. Thermogravimetric (TGA-DTG) curve of pristine CHP film and bio nanocomposite films shows three distinct stage of decomposition. In the first stage the weight loss of 15% was observed at the temperature ranging from

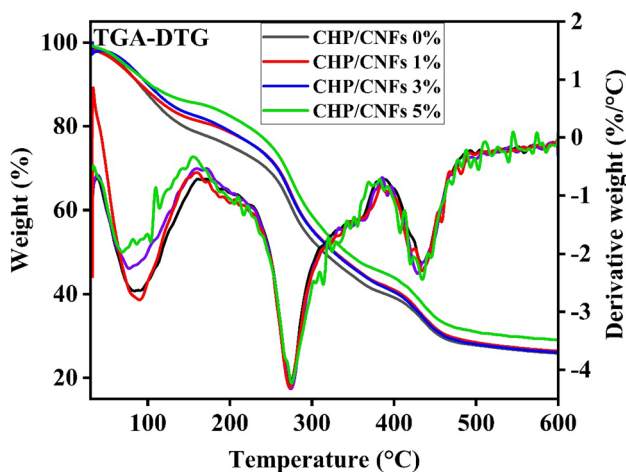


Fig. 11 TGA and DTG thermogram of CHP/CNFs 0%, CHP/CNFs 1%, CHP/CNFs 3%, CHP/CNFs 5% bio nanocomposite film

50 to 160 °C with a peak at 90 °C, which is attributed to the evaporation of moisture present in the composite material. In the second stage the weight loss of 56% was observed at temperature ranging from 160 to 380 °C with a peak at 273 °C relate to the structural degradation of chitosan and during the third stage of degradation the weight loss of 69% was observed at temperature ranging from 390 to 490 °C with a peak at 434 °C due to the degradation of the PVP. The initial weight loss in the region of 50–160 °C was decreased with the addition of CNFs, suggesting the uniform dispersion of CNFs in CHP matrix. Thus, decreasing the absorption of moisture by the nanocomposite film. From results, it confirmed that with the addition of CNFs in CHP matrix prepared bio nanocomposite films did not show much difference in degradation temperature [38, 43]. However, the prepared bio nanocomposite films are thermally stable and suitable for packaging application.

### Mechanical Analysis

The average value of tensile strength and young’s modulus of CHP/CNFs having 0%, 1%, 3%, and 5% cellulose nanofibers are shown in Fig. 12. The mechanical property of bio nanocomposite film depends on many factors such as orientation, content and size of the fiber as well as the interaction between fiber and polymer matrix. The increase in tensile strength and young’s modulus of bio nanocomposite film with the incorporation of CNFs was due to its small size and uniform distribution in polymer matrix which leads to minimizing of pours in the composite and failure propagation points [22]. The tensile strength and young’s modulus of bio nanocomposite film increased up to 32.44 MPa and 2139 MPa with the addition of CNFs as compared to pristine CHP film having tensile strength and young’s modulus of 23.42 MPa and 1188 MPa, respectively. This increase in tensile

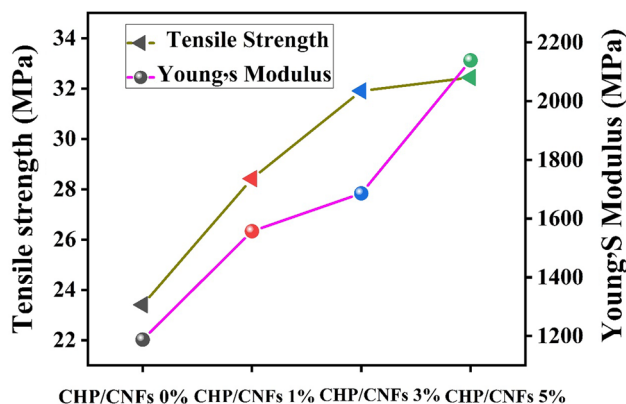
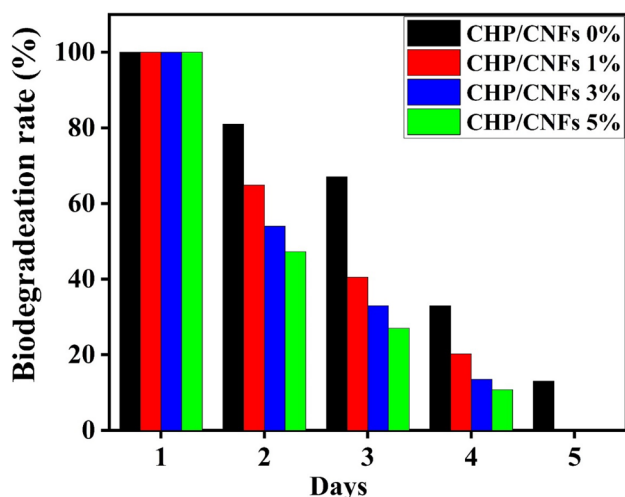


Fig. 12 Tensile strength and young’s modulus of CHP/CNFs 0%, CHP/CNFs 1%, CHP/CNFs 3%, CHP/CNFs 5% bio nanocomposite film



**Fig. 13** Biodegradability study of CHP/CNFs 0%, CHP/CNFs 1%, CHP/CNFs 3%, CHP/CNFs 5% bio nanocomposite film

strength and young's modulus shows the homogeneous distribution of CNFs in the film and also indicated the strong interaction between cellulose nanofibers and CHP matrix. Thus, the tensile strength results suggested the improvement in mechanical property of bio nanocomposite film with the addition of CNFs.

### Biodegradability Analysis

The weight loss in term of Biodegradation property of pristine CHP film and CNFs reinforced bio nanocomposite film is shown in Fig. 13. The addition of CNFs in CHP matrix enhances the weight loss at tremendous rate and the prepared nanocomposite film is eroded from solid to an aqueous phase. This shows that by providing the natural condition nanocomposite will easily degrade [42]. This biodegradable property makes it potential material to be used as biodegradable plastic for packaging application.

### Conclusions

Cellulose nanofibers (CNFs), with the dimensions of 9–11 nm and 100–200 nm were obtained from jute fiber by directly oxidizing it with  $\text{HNO}_3$ - $\text{NaNO}_2$  mixture. The bio nanocomposite film was developed by introducing various concentration of CNFs into CHP matrix using an eco-friendly solvent casting method. From SEM microgram of bio nanocomposite film efficient and homogeneous dispersion of CNFs into CHP matrix was observed which resulted in improvement of the properties of developed nanocomposite film. The developed bio nanocomposite films possessed higher mechanical property, flexibility and transparency as

compared to pristine CHP film. Further higher crystallinity of CNFs and dense composite structure of developed film leads to reduce the water vapor transmission rate and increase the oxygen barrier properties. Moreover, biodegradability study shows the degradation of bio nanocomposite films at a faster rate than pristine CHP film. Results from the study indicated that the  $\text{HNO}_3$ - $\text{NaNO}_2$  oxidized CNFs addition into CHP matrix produced a green, flexible and transparent bio nanocomposite film which might be suitable for packaging food products.

**Acknowledgements** One of the authors Ritesh Kumar, is grateful to GGSIP University, New Delhi for providing financial assistance in the form of Indraprastha Research Fellowship (IPRF) vide letter no. GGSIPU/DRC/Ph.D./2018/1220. We would also like to thank the lab staff of BTL-311 (USBAS) for their invaluable support and guidance to make this research successful. The authors would also like to thank All India Institute of Medical Sciences (AIIMS) for TEM facility and Prof. B.R Mehta (TFL, Indian Institute of technology, New Delhi) to provide characterization facility during course of investigation.

### Compliance With Ethical Standards

**Conflict of interest** There are no conflicts of interest.

### References

1. Wang H, Qian J, Ding F (2018) *J Agric Food Chem* 66:395–413
2. Johar N, Ahmad I, Dufresne A (2012) *Ind Crops Prod* 37:93–99
3. Gopi S, Amalraj A, Jacob J, Kalarikkal N, Thomas S, Guo Q (2018) *New J Chem* 42:5117–5127
4. Gopi S, Amalraj A, Kalarikkal N, Zhang J, Thomas S, Guo Q (2018) *Mater Sci Eng C* 97:723–729
5. Jacob J, Haponiuk JT, Thomas S, Peter G, Gopi S (2018) *Fibers* 6:79–90
6. Amalraj A, Jude S, Varma K, Jacob J, Gopi S, Oluwafemi SO, Thomas S (2017) *Mater Sci Eng C* 75:359–367
7. Nascimento P, Marim R, Carvalho G, Mali S (2016) *Mater Res* 19:167–174
8. Malini M, Thirumavalavan M, Yang W, Lee J, Annadurai G (2015) A versatile chitosan / ZnO nanocomposite with enhanced antimicrobial properties. *Int J Biol Macromol* 80:121–129
9. Cheng Z, Teoh SH (2004) *Biomaterials* 25:1991–2001
10. Kargazadeh H et al (2018) *Prog Polym Sci* 87:197–227
11. Rhim JW, Ng Perry KW (2007) *Crit Rev Food Sci Nutr* 47:411–433
12. Jacob J, Haponiuk JT, Thomas S, Gopi S (2018) *Mater Today Chem* 9:43–55
13. Jacob J, Peter G, Thomas S, Haponiuk JT, Gopi S (2019) *Int J Biol Macromol* 129:370–376
14. Gopi S, Amalraj A, Jude S, Thomas S, Guo Q (2019) *J Taiwan Inst Chem Eng* 96:664–671
15. Hossain MS, Iqbal A (2014) *J Bangladesh Agril Univ* 12:153–160
16. Lin S, Chen L, Huang L, Cao S, Luo X, Liu K (2015) *Ind Crops Prod* 70:395–403
17. Thakur VK, Voicu SI (2016) *Carbohydr Polym* 146:148–165
18. Lewandowska K, Sionkowska A, Kaczmarek B, Furtos G (2014) *Mol Cryst Liq Cryst* 590:193–198
19. Alver E, Metin A, Çiftçi H (2014) *J Inorg Organomet Polym Mater* 24:1048–1054

20. Basha SKS, Rao MC (2018) *Polym. Bull* 75:3641–3666
21. Yeh JT, Chen CL, Huang KS, Nien YH, Chen JL, Huang PZ (2006) *J Appl Polym Sci* 101:885–891
22. Poonguzhali R, Basha SK, Kumari VS (2018) *Int J Biol Macromol* 112:1300–1309
23. Li J, Zivanovic S, Davidson PM, Kit K (2010) *Carbohydr Polym* 79:786–791
24. Neves MA (2016) *Food Sci.* 2:1–7
25. Zhu H et al (2012) *Desalination* 286:41–48
26. Chirayi CJ, Mathew L, Thomas S (2014) *Rev Adv Mater. Sci* 37:20–28
27. Sumaiyah B, Wirjosentono K, Nasution MP, Gea S (2014) *Int J PharmTech Res* 6:814–820
28. Gopi S, Amalraj A, Varma K, Jude S, Reddy PB, Divya C, Haponiuk JT, Thomas S (2018) *Int J Polym Mater Polym Biomater* 67:581–588
29. Gopi S, Amalraj A, Jude S, Benson KT, Balakrishnan P, Haponiuk JT, Thomas S (2019) *J Macromol Sci Part A* 56:327–340
30. Gopi S, Amalraj A, Jude S, Varma K, Sreeraj TR, Haponiuk JT, Thomas S (2017) *Mater Sci Eng C* 81:20–31
31. EI-Miri N et al. (2015) *Carbohydr Polym* 129:156–167
32. Dehnad D, Mirzaei H, Emam-djomeh Z, Jafari S (2014) *Carbohydr Polym* 109:148–154
33. Tibolla H, Pelissari FM, Martins JT, Vicente AA, Menegalli FC (2018) *Food Hydrocoll* 75:192–201
34. Soni B, Barbary E, Schilling MW, Mahmoud B (2016) *Carbohydr Polym* 151:779–789
35. Sharma PR, Joshi R, Sharma SK, Hsiao BS (2017) *Biomacromol* 18:2333–2342
36. Kumar R, Kumari S, Surah SS, Rai B, Kumar R, Sirohi S, Kumar G (2019) *Mater Res Express* 6:105601
37. EI-Hefian EA, Nasef MM, Yahaya AH (2012) *J Chem* 9: 1431–1439
38. Hasan A, Waibhaw G, Tiwari S, Dharmalingam K, Shukla I, Pandey LM (2017) *J Biomed Mater Res Part A* 105:2391–2404
39. Poonguzhali R, Basha SK, Kumari VS (2018) *Polym Plast Technol Eng* 57:1400–1410
40. Huang L et al (2018) *AIP Adv* 8:025116
41. Poonguzhali R, Basha SK, Kumari VS (2017) *Int J Biol Macromol* 105:111–120
42. Samzadeh-kermani A, Esfandiary N (2016) *Adv Nanopart* 5:18–26
43. Devi MP, Sastry TP, Meignanalakshmi S (2012) *J Pharm* 2:21–32

**Publisher's Note** Springer Nature remains neutral with regard to jurisdictional claims in published maps and institutional affiliations.